Nanoscale



COMMUNICATION

View Article Online



Cite this: DOI: 10.1039/d0nr08605c

Received 4th December 2020, Accepted 30th March 2021 DOI: 10.1039/d0nr08605c

rsc.li/nanoscale

Mechanochemical properties of DNA origami nanosprings revealed by force jumps in optical tweezers†

Deepak Karna, [©] ^a Wei Pan, ^a Shankar Pandey, ^a Yuki Suzuki [©] ^{b,c} and Hanbin Mao [©] *

By incorporating pH responsive i-motif elements, we have constructed DNA origami nanosprings that respond to pH changes in the environment. Using an innovative force jump approach in optical tweezers, we have directly measured the spring constants and dynamic recoiling responses of the DNA nanosprings under different forces. These DNA nanosprings exhibited 3 times slower recoiling rates compared to duplex DNA backbones. In addition, we observed two distinct force regions which show different spring constants. In the entropic region below 2 pN, a spring constant of ~ 0.03 pN nm⁻¹ was obtained, whereas in the enthalpic region above 2 pN, the nanospring was 17 times stronger (0.5 pN nm⁻¹). The force jump gave a more accurate measurement on nanospring constants compared to regular force ramping approaches, which only yielded an average spring constant in a specific force range. Compared to the reported DNA origami nanosprings with a completely different design, our nanospring is up to 50 times stiffer. The drastic increase in the spring constant and the pH responsive feature allow more robust applications of these nanosprings in many mechanobiological processes.

Introduction

DNA origami structures¹⁻⁶ have provided versatile tools in a wide variety of applications including drug delivery, sensing, and fabrication of materials with nanometer precision. Many of these applications exploit the mechanical properties of origami structures. Force manipulation tools such as Atomic Force Microscopy (AFM), optical tweezers and magnetic tweezers⁷⁻¹¹ have been used to characterize the mechanical

properties of DNA origami structures. In most cases, single-molecule force spectroscopy has been employed 12,13 to reveal the stress-strain behaviors of DNA nanoassemblies. In a typical strategy, a DNA origami structure is attached between two surfaces. One of the surfaces is then moved away from the other by using a nanomanipulator employed in the force manipulating instruments. During this process, the tensile force in the DNA origami structure varies. Such a variation causes a property change in the nanoassembly, which will be monitored in real time.

However, this method is difficult to reveal the dynamic structural changes in DNA origami nanoassemblies. Recently, Shih and co-workers have designed an elegant DNA origami nanodevice, DNA nanospring. Similar to macroscopic springs, this nanospring extends and contracts in response to external forces. Using force–extension curves, the spring constant of the DNA nanospring has been estimated as 0.01 pN nm⁻¹, a value that is suboptimal for many mechanochemical and mechanobiological processes. Dur previous finding has indicated that integrin heterodimers require about 25 pN for their clustering and declustering activities which require a nanospring having a stiffer spring constant for the study. In addition, the dynamic response of the nanospring is difficult to be measured by these force–extension curves reported by Shih and co-workers.

In this work, we prepared DNA origami nanosprings with stronger spring constants. These nanosprings have a unique feature to respond to external cues such as pH. This feature has been achieved by incorporating a pH sensitive element, i-motif, in the junction between adjacent DNA origami modules. At acidic pH (pH \sim 5.5), the folding of the i-motif induces a curvature in the origami modules, which leads to coiled nanosprings. At neutrality, the unfolded i-motif relaxes the curvature, causing an uncoiled conformation of the origami templates. We applied innovative force jump methods to follow the coiling and uncoiling of the nanosprings at different pH. This allowed us to reveal that the spring constants of the nanosprings are dependent on the force exerted

^aDepartment of Chemistry and Biochemistry, Kent State University, Kent, Ohio, 44242, USA. E-mail: hmao@kent.edu

^bFrontier Research Institute for Interdisciplinary Sciences, Tohoku University, 6-3 Aramaki-aza Aoba, Aoba-ku, Sendai, 980-8578, Japan

^cDepartment of Robotics, Graduate School of Engineering, Tohoku University, 6-6-01 Aramaki-aza Aoba, Aoba-ku, Sendai, 980-8579, Japan

[†]Electronic supplementary information (ESI) available. See DOI: 10.1039/d0nr08605c

Communication Nanoscale

on the DNA nanoassemblies. The nanosprings showed 0.03-0.5 pN nm⁻¹ spring constants at pH 5.0, which is about 50 times stiffer than previously designed nanosprings. 14 We anticipate these pH responsive nanosprings can be used to investigate pH-dependent mechanobiological processes such as cell migration.

Results and discussion

Our nanospring (Fig. 1a) was assembled from a circular ssDNA template (p8064) by a DNA origami approach. 16 The DNA origami backbone contained 37 modules. A bridge was inserted between two neighboring modules. The bridge strand comprised a human telomeric C-rich DNA sequence 5'-CCCTAACCCTAACCC-3', which was extended with staple sequences that were anchored into each module. Upon the i-motif formation in the DNA sequence at pH 5.0, the bridge strand contracts, leading to the bending of neighboring modules. The propagation of such a bending in the entire origami backbone transformed the DNA nanoassembly from linear to a spring conformation at acidic pH (Fig. 1a). When the i-motif sequence was replaced by 21 thymines (21T), no coiling was observed (Fig. S2†). In another control, when the i-motif bridge sequence was replaced by two thymines (2T-NS), the nanospring attained a coiled form irrespective of pH (see Fig. S3 and S4†). All these observations verified that pH responsive i-motif bridges between neighboring modules are the driving force for the coiling of nanosprings.

Next, we used optical tweezers to analyze the mechanical properties of the as-synthesized nanosprings. To this purpose, the two ends of a nanospring were respectively ligated to two dsDNA handles (Fig. 1a, and see the ESI† for details), which were labeled separately with digoxigenin and biotin at their free ends. This design facilitated the tethering of the nanospring to the optically trapped polystyrene beads that were respectively coated with digoxigenin antibody and streptavidin via affinity linkages (Fig. 1b). 18 After tethering of the nanospring, the force-ramping experiments were conducted at a loading rate of 5.5 pN s⁻¹ (measured from 10-40 pN) in a fourchanneled microfluidic chamber at room temperature. The middle two channels of the chamber contained 5 mM MES buffers supplemented with 15 mM MgCl₂ and 1 mM EDTA at pH 5.0 and 7.4, respectively. This experimental setup provided a platform to measure the mechanical properties of individual DNA nanosprings over varying pH of 5.0 and 7.4.

At pH 5.0, hysteresis between the stretching and relaxing force-extension (F-X) curves was observed in the mechanical

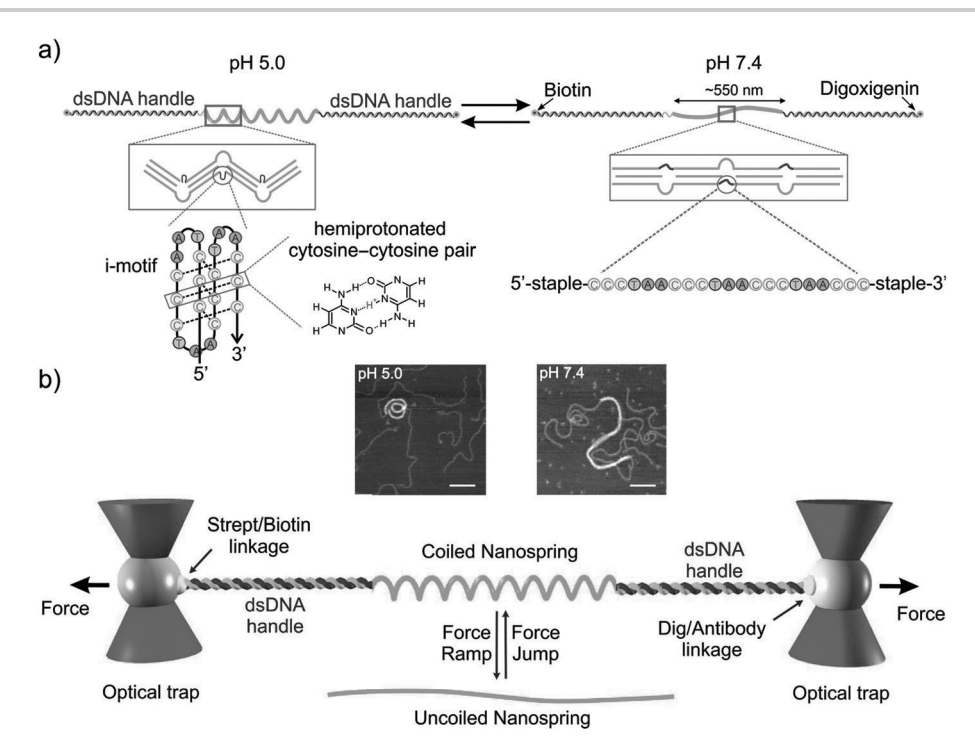


Fig. 1 Design and characterization of a pH-responsive DNA origami nanospring. (a) pH-Responsive transformation of a linear shape into a spring conformation through the bending of adjacent origami modules. Each bridge between two neighboring modules (represented by red circles) contains a C-rich human telomeric DNA sequence, 5'-CCCTAACCCTAACCCTAACCC-3'. The DNA strand forms an i-motif at pH 5.0, which causes the bending of neighboring modules. This, in turn, induces the nanospring formation. A hemiprotonated cytosine-cytosine pair is depicted next to the i-motif structure. (b) Laser tweezers set up where an i-motif-forming DNA nanospring ligated to two dsDNA handles. One dsDNA handle labeled with biotin is attached to the streptavidin-coated bead, while the other handle labeled with digoxigenin is attached to the digoxigenin antibodycoated polystyrene bead. AFM images on top show the conformations of the nanosprings attached with two long DNA handles on both ends (red arrows) at pH 5.0 and 7.4. Scale bar: 100 nm. More AFM images are shown in Fig. S1.†

Nanoscale Communication

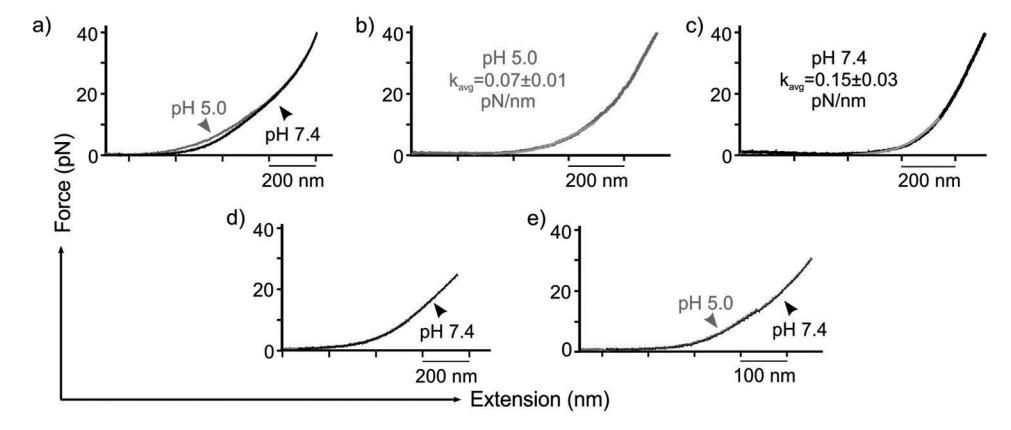


Fig. 2 (a) Force–extension (F-X) curves at pH 5.0 and 7.4 for the i-motif containing nanospring. Fitting of F-X curves to calculate the spring constants of nanosprings at (b) pH 5.0 and (c) pH 7.4. F-X traces for the (d) 2T-nanospring and (e) duplex DNA. The red and black traces represent the stretching and relaxing processes, respectively. More F-X traces for the i-motif containing nanosprings are shown in Fig. S6.†

pulling of the nanospring with the i-motif bridges (Fig. 2a). In contrast, the hysteresis disappeared at pH 7.4. Such a difference suggested that the nanospring may present different conformations under the two pH conditions. At acidic pH, the i-motif forming sequences in the bridges of adjacent piers may fold into i-motif structures. The compact topology of each folded domain brings two neighboring modules closer, causing the coiling of the nanospring. When force increases, the end-to-end distance of the DNA origami becomes longer due to the physical stretching of nanosprings. At pH 5.0, when force is ~11 pN, the i-motif starts to unfold until a complete unfolding is reached at ~35 pN (Fig. S5(a)†). 17,18 This will further increase the end-to-end distance. The F-X histogram (Fig. S5(a)†) also indicates that an average force of ~25 pN is needed to unfold the i-motif. Upon reducing the tension in the origami construct, the slow folding of the i-motif prevents the fast recoiling of the nanospring, leading to hysteresis between the stretching and relaxing F-X curves at acidic pH. At pH 7.4, the i-motif is not formed even at low force regimes, leading to reversible F-X curves since the nanospring is uncoiled at neutrality during the experiment. With no such hysteresis observed in the F-X traces of "2T-NS" and "DNA only" (DNA hairpin) as shown in Fig. 2d and e, respectively, we confirm that hysteresis is entirely due to the formation and dissolution of the i-motif at different pH.

To estimate the spring constant of the nanospring, we developed a model (see Fig. S7†) to delineate the response of the extension of the entire origami construct against force. We used the extensible worm-like-chain (WLC) model¹⁹ for analyzing the behavior of the dsDNA handles, and Hooke's law for analyzing that of the nanospring. To rule out the effect of the i-motif unfolding (which started at ~11 pN, Fig. S5(a)†) on the elastic behavior of the system, we used this model to fit the F-X curves below 11 pN at pH 5.0 (Fig. 2b) and pH 7.4 (Fig. 2c, see Table S1†). The fitting allowed us to retrieve spring constants of 0.07 \pm 0.01 and 0.15 \pm 0.03 pN nm⁻¹ for the i-motif containing nanosprings at pH 5.0 and 7.4, respectively. Since the nanospring is coiled at pH 5.0 and the origami structure

remains uncoiled at pH 7.4, it is clear that such a nanospring at pH 5.0 has a softer spring constant compared to that of the origami backbones tested at pH 7.4.

In another approach, we directly characterized the mechanical properties of the nanosprings via force-jump methods in optical tweezers.20 First, the tethered DNA structures were stretched to an initial force of 25 pN. The force was then suddenly reduced to a small level (0.5-9 pN) within 10 ms ²⁰ while the recoiling event was monitored (Fig. 3a) by measuring the distance between the stretched state and the completely recoiled equilibrium state at a low force (Δd) over a period of time (t). This measurement provided the recoiling rate $(\Delta d/t)$ for each nanostructure. As seen in Fig. 3b, the nanosprings (both "2T-NS" and "coiled") showed much longer recoiling distances compared to those of their linear counterparts (both "DNA only" and "uncoiled"). The inherent elasticity of the duplex DNA caused the DNA handles to be shortened quickly by this force jump-down process (see "DNA-only" in Fig. 3b; the recoiling rate: 80 ± 5 nm s⁻¹ and see Fig. S7† for elucidation). The i-motif containing DNA nanosprings, however, showed much slower recoiling at pH 5.0 ("Coiled" in Fig. 3b; the recoiling rate: $24 \pm 3 \text{ nm s}^{-1}$) likely due to the fact that they had a long distance to travel from the extended to coiled states and they were more flexible than dsDNA. The slower rate can also be ascribed to the slow refolding of some unfolded i-motif structures in the bridge regions. As expected, the i-motif containing DNA origami that did not form coils at pH 7.4 ("Uncoiled" in Fig. 3b; the recoiling rate: $57 \pm 10 \text{ nm s}^{-1}$) showed a speed similar to that of the dsDNA ("DNA-only"), since both structures (the DNA origami backbone at pH 7.4 and the duplex DNA at pH 7.4) have stronger elasticities than the coiled nanospring. As a control, we also performed the force-jump experiments on the DNA origami nanospring with the T2 bridge linkers ("2T-NS" in Fig. 3) at pH 7.4. We found that the recoiling rate for the 2T-NS (29 \pm 6 nm s⁻¹) was similar to that of the "Coiled" origami, which is expected since both constructs assume a coiled nanospring conformation at a low force (Fig. S8(a) and S3†).

Communication

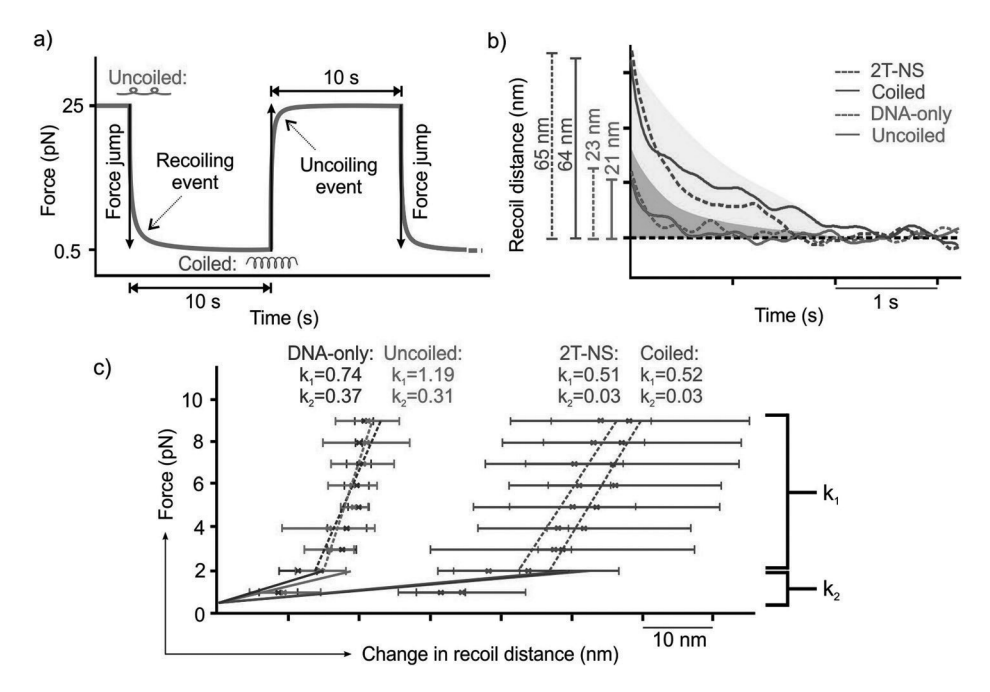


Fig. 3 Properties of the DNA nanosprings revealed by force-jump approaches. (a) Schematic representation of the force vs. time plot. (b) Recoiling distance over time after a force jump from 25→0.5 pN. Note that the kinetics of the recoiling is the average rate from time 0 (as soon as the final force is reached) to the fully recoiled state. (c) Measurement of the spring constants based on Hooke's law. Error bars represent the standard deviations of 3 molecules. Ratio of the change in the final force vs. the change in the recoiling distance (with respect to the 0.5 pN value) gives the spring constant. "Coiled" and "Uncoiled" refer to the i-motif containing origami nanospring at pH 5.0 and pH 7.4, respectively. "2T-NS" and "DNAonly" refer to the 2T containing origami nanospring and a construct that contains only two dsDNA handles (see the ESI† for details), respectively, at pH 7.4.

For the calculation of spring constants as shown in Fig. 3c, the change in recoil distances was calculated based on the difference between the stretched state and the recoiled state observed at a specific recoiling force. These changes in the recoiling distance were plotted with respect to the recoiling forces upon which two linear fits were made: one below 2 pN to 0.5 pN and another above 2 pN to 9 pN. The slopes of these linear fits (revealed by force per unit extension or Hooke's law) provided the spring constants over the respective force regimes.

The flexibility of the nanosprings was well supported by the spring constants estimated by Hooke's law (i.e. change in force per unit change in extension in the nanospring) in these rapid recoiling experiments. Two sets of spring constants bifurcated at 2 pN are clearly seen in Fig. 3c. This observation can be ascribed to the higher entropic contribution to coiling at a lower force (<2 pN), while higher enthalpic contribution to the backbone stretching above 2 pN. Entropic elasticity is experienced when the persistence length of a polymer is much smaller than the contour length of the polymer. 21 At a low force, the persistence length of the DNA (~50 nm) is much smaller than the contour length of the DNA handles and the DNA nanospring used here, so, the entropic contribution is expected for the elasticity. However, at a higher force, the chemical bonds become stretched and hence the elasticity is contributed by enthalpy.²² This difference in their conformation above/below 2 pN results in differential spring constants. At the final force above 2 pN, the backbone of the nano-

spring was still at some stretched state, leading to inaccurate spring constant estimation for the nanosprings resting near their native length (F = 0 pN), which gave a spring constant of $0.03 \pm 0.01 \text{ pN nm}^{-1}$ for the coiled DNA nanosprings ("Coiled" at pH 5.0). Since the 2T-NS construct also formed the coiled nanospring (Fig. S3 and S4†), it gave an identical spring constant $(0.03 \pm 0.01 \text{ pN nm}^{-1})$ as expected. In comparison, spring constants of 0.37 \pm 0.03 and 0.31 \pm 0.02 pN nm⁻¹ for the "DNA-only" construct and uncoiled nanospring were obtained respectively at pH 7.4. The smaller spring constants of the coiled nanosprings with respect to that of dsDNA ("DNA-only") or the origami backbone ("Uncoiled") imply that when an external force was applied, the coiled nanosprings formed at pH 5.0 imposed greater extension variation compared to the dsDNA or uncoiled origami nanosprings. During the rapid recoiling process, the i-motif may not have time to refold, this explains the deviation in the spring constants measured by the force jump method (Fig. 3) and those obtained from the fitting of the force-extension curves (Fig. 2). In addition, the deviation can also be ascribed to different force ranges used in these two methods. While the force-extension curves measured the average spring constant from 0-11 pN, the force jump approach was more accurate in the depiction of spring constants at different force ranges.

Compared to the origami nanosprings prepared in the Shih lab where coils were formed by mechanical strains due to the insertion of extra base pairs in the 2-helix bundles, 14 our nanoNanoscale Communication

springs have the unique advantages of accommodating environmentally sensitive functional groups in the bridge regions as well as 50 times stiffer spring constants. While the stronger spring constants provide a robust material to interact with cells without disrupting the nanocoils, the facile incorporation of functional groups allows flexible responses of our origami nanoassembly to environmental cues such as pH variation in the extracellular matrix (ECM).²³

Conclusions

In summary, using optical tweezers, we successfully characterized the mechanochemical properties of DNA origami nanosprings in the pH range of 5.0-7.4. Unlike the conventional spring constant measurement in which the tensile force of a nanospring is continuously monitored over the extension of the nanodevice, here we rapidly perturbed the tensile force in nanosprings while following the response of the nanospring extensions. While the former method only provided an average spring constant over a wide force range, our new method allowed to reveal the spring constants over variable force ranges. Indeed, we found two distinct spring constants bifurcated at 2 pN for this DNA origami nanospring. With the burgeoning development of DNA nanoassemblies, we anticipate that our novel method would provide a better mechanistic description of DNA devices that have applications ranging from study of motor proteins to formulating origami nanodevices.

Author contributions

HM conceptualized the project. YS synthesized the DNA origami. HM supervised the mechanical characterization of the nanosprings. DK and WP performed the mechanical characterization. DK and SP performed the i-motif force jump experiments. HM, DK and YS co-wrote the manuscript.

Conflicts of interest

There are no conflicts to declare.

Acknowledgements

HM thanks the NIH (R01 CA236350 for construct preparation) and the NSF (CBET-1904921 for nanospring characterization) for support. YS thanks the Japan Society for the Promotion of Science (JSPS) Grant-in-Aid for Scientific Research (KAKENHI; grant numbers 18K19831, 18KK0139 and 19H04201).

References

1 F. Hong, F. Zhang, Y. Liu and H. Yan, DNA Origami: Scaffolds for Creating Higher Order Structures, *Chem. Rev.*, 2017, 117(20), 12584–12640.

2 S. M. Douglas, H. Dietz, T. Liedl, B. Högberg, F. Graf and W. M. Shih, Self-assembly of DNA into nanoscale three-dimensional shapes, *Nature*, 2009, **459**(7245), 414–418.

- 3 S. M. Douglas, I. Bachelet and G. M. Church, A Logic-gated Nanorobot for Targeted Transport of Molecular Payloads, *Science*, 2012, **335**, 831–834.
- 4 Y. Ke, C. Castro and J. H. Choi, Structural DNA Nanotechnology: Artificial Nanostructures for Biomedical Research, *Annu. Rev. Biomed. Eng.*, 2018, **20**(1), 375–401.
- 5 H. Dietz, S. M. Douglas and W. M. Shih, Folding DNA into twisted and curved nanoscale shapes, *Science*, 2009, 325(5941), 725–730.
- 6 D. Han, S. Pal, J. Nangreave, Z. Deng, Y. Liu and H. Yan, DNA Origami with Complex Curvatures in Three-Dimensional Space, *Science*, 2011, 332, 342–346.
- 7 A. Ashkin, J. M. Dziedzic, J. E. Bjorkholm and S. Chu, Observation of a single-beam gradient force optical trap for dielectric particles, *Opt. Lett.*, 1986, 11(5), 288–290.
- 8 A. Ashkin, Optical Trapping and Manipulation of Neutral Particles using Lasers, *Proc. Natl. Acad. Sci. U. S. A.*, 1997, 4853–4860.
- 9 T. R. Strick, J.-F. Allemand, D. Bensimon, A. Bensimon and V. Croquette, The Elasticity of a Single Supercoiled DNA Molecule, *Science*, 1996, 271, 1835–1837.
- 10 E. Winfree, F. Liu, L. A. Wenzler and N. C. Seeman, Design and self-assembly of two-dimensional DNA crystals, *Nature*, 1998, **394**(6693), 539–544.
- 11 H. B. Li, M. Rief, F. Oesterhelt and H. E. Gaub, Single-molecule force spectroscopy on Xanthan by AFM, *Adv. Mater.*, 1998, **10**(4), 316–319.
- 12 M. Rief, H. Clausen-Schaumann and H. E. Gaub, Sequence-dependent mechanics of single DNA molecules, *Nat. Struct. Biol.*, 1999, **6**, 346–349.
- 13 V. Birkedal, M. Dong, M. M. Golas, B. Sander, E. S. Andersen, K. V. Gothelf, F. Besenbacher and J. Kjems, Single molecule microscopy methods for the study of DNA origami structures, *Microsc. Res. Tech.*, 2011, 74(7), 688– 698.
- 14 M. Iwaki, S. F. Wickham, K. Ikezaki, T. Yanagida and W. M. Shih, A programmable DNA origami nanospring that reveals force-induced adjacent binding of myosin VI heads, *Nat. Commun.*, 2016, 7(1), 13715.
- 15 V. Vogel, Unraveling the Mechanobiology of Extracellular Matrix, *Annu. Rev. Physiol.*, 2018, **80**(1), 353–387.
- 16 D. Karna, M. Stilgenbauer, S. Jonchhe, K. Ankai, I. Kawamata, Y. Cui, Y.-R. Zheng, Y. Suzuki and H. Mao, Chemo-Mechanical Modulation of Cell Motions Using DNA Nanosprings, *Bioconjugate Chem.*, 2021, 32(2), 311–317.
- 17 S. Dhakal, J. D. Schonhoft, D. Koirala, Z. Yu, S. Basu and H. Mao, Coexistence of an ILPR i-Motif and a Partially Folded Structure with Comparable Mechanical Stability Revealed at the Single-Molecule Level, *J. Am. Chem. Soc.*, 2010, 132(26), 8991–8997.
- 18 S. Jonchhe, S. Pandey, T. Emura, K. Hidaka, M. A. Hossain, P. Shrestha, H. Sugiyama, M. Endo and H. Mao, Decreased water activity in nanoconfinement contributes to the

Communication Nanoscale

- folding of G-quadruplex and i-motif structures, *Proc. Natl. Acad. Sci. U. S. A.*, 2018, **115**(38), 9539–9544.
- 19 C. G. Baumann, V. A. Bloomfield, S. B. Smith, C. Bustamante, M. D. Wang and S. M. Block, Stretching of Single Collapsed DNA Molecules, *Biophys. J.*, 2000, 78(4), 1965–1978.
- 20 D. Koirala, S. Dhakal, B. Ashbridge, Y. Sannohe, R. Rodriguez, H. Sugiyama, S. Balasubramanian and H. Mao, A Single-Molecule Platform for Investigation of Interactions between G-quadruplexes and Small-Molecule Ligands, *Nat. Chem.*, 2011, 3, 782–787.
- 21 M. D. Wang, H. Yin, R. Landick, J. Gelles and S. M. Block, Stretching DNA with optical tweezers, *Biophys. J.*, 1997, 72(3), 1335–1346.
- 22 C. Bouchiat, M. D. Wang, J. F. Allemand, T. Strick, S. M. Block and V. Croquette, Estimating the persistence length of a worm-like chain molecule from force-extension measurements, *Biophys. J.*, 1999, 76(1), 409–413.
- 23 I. F. Tannock and D. Rotin, Acid pH in Tumors and Its Potential for Therapeutic Exploitation, *Cancer Res.*, 1989, 49(16), 4373–4384.